02,19

Study of superconducting transmission lines based on NbTiN/Al and pumping of Nb/AlN/NbN SIS junctions in the frequency range above 1 THz

© N.V. Kinev[1], A.M. Chekushkin[1], F.V. Khan[1,2], K.I. Rudakov[1,3], N.N. Kotova[1,2], V.P. Koshelets[1]

[1] Kotelnikov Institute of Radio Engineering and Electronics, Russian Academy of Sciences, Moscow, Russia
[2] Moscow Institute of Physics and Technology (National Research University), Dolgoprudny, Moscow Region, Russia
[3] Astro Space Center of P.N. Lebedev Physical Institute of the Russian Academy of Sciences, Moscow, Russia

E-mail: nickolay@hitech.cplire.ru

Received April 18, 2024
Revised April 18, 2024
Accepted May 8, 2024

Superconducting transmission lines based on NbTiN/Al were studied as rf lines for operation at frequencies up to 1.1 THz. Circuits for studying damping in thin-film structures consisting a receiving slot THz antenna, a set of NbTiN/Al microstrip transmission lines, and two THz detectors based on the „superconductor–insulator–superconductor" Nb/AlN/NbN tunnel junction matched to the line were numerically simulated and fabricated. An experiment was carried out to register an external source signal (backward wave oscillator) at a frequency of about 1.1 THz, demonstrating the successful operation of the developed NbTiN/Al transmission lines at frequencies above 1 THz, where traditional Nb-based transmission lines are not applicable. The analysis of the heating effect is made when the detector is affected by external rf signal, which leads to a powerful pumping of the tunnel junction.

Keywords: terahertz detectors, SIS junctions, thin films, thermal effect, superconducting gap.

DOI: 10.61011/PSS.2024.07.58965.26HH

1. Introduction

The high-sensitive terahertz (THz) detectors are currently widely popular in a whole bunch of spheres such as communication, biomedicine, astrophysical research, molecular spectroscopy [1–3]. The cryogenic superconductor detectors are currently the most sensitive ones in a THz-band [4], where one of the most common types is a tunnel junction „superconductor–insulator–superconductor" (SIS). Most of the existing tunnel-junction based receiving systems use niobium (e.g., $Nb/AlO_x/Nb$) or niobium nitride (e.g., Nb/AlN/NbN) operating at 4.2 K Helium boiling temperature as the SIS junction electrodes. For these junctions the most conventional signal transfer lines are the thin niobium films fabricated using the same processes as for the tunnel junctions, while some elements being formed in a common vacuum cycle. Their maximum operating frequency is about 750 GHz, above which the film losses may occur due to a fundamental limitation resulting from the energy slot of Δ superconductor, according to Mattis–Bardeen theory [5]. In systems operating with frequencies under 1 THz and above it is required to use higher frequency signal transfer lines made of materials of higher Δ value. The most suitable for such tasks are the NbTiN signal transfer lines with operating frequencies above 1.4 THz [6–7]. This paper outlines the processes of development, fabricating and study of the superconductor integrated circuits to get an insight on the characteristics of NbTiN/Al signal transfer lines with operating frequencies above 1 THz.

The study of pumping of SIS detectors Nb/AlN/NbN in NbTiN/Al signal transfer lines with the signal from backward-wave oscillator (BWT or BWO) at frequencies of up to 1.1 THz was described in [8], however, no numerical analysis was carried out. Defining the absolute power absorbed by the SIS junction in the signal transfer line is a complex task where, among other things, it is required to take into account the influence of thermal effect of emission acting on the junction. The power is commonly estimated by a computational modeling of current-voltage curves under signal of certain amplitude and frequency [8–10] and their comparison with experimentally measured current-voltage curves. Here, as a result of thermal effect from the action of outer signal the „gap voltage" V_g of SIS junction [9,11] is changing, which should be known in the computational modeling of the current-voltage curves and power estimate in absolute units. Therefore, to make it possible to study the signal transfer lines not only in terms of quality, but in terms of quantity as well, this paper used a method of defining the V_g SIS junction when exposed to the outer signal. Results of modeling and production of prototype samples are given in section 2. The experimental results for recording of THz-signals are given in section 3. The analysis of thermal effect of pumping and defining the value V_g of SIS detectors are given in section 4.

2. Computational modeling (simulation) and its results

We have developed and simulated the topology of an integrated circuit containing Nb/AlN/NbN-based SIS junctions included in THz signal transfer line with NbTiN as lower electrode and Al as upper electrode acting as detectors of outer THz-signal. The circuit topology is shown in Figure 1 and consists of the entrance slot antenna located in the lower NbTiN electrode of the integral structure, two detectors made on the basis of a twin SIS junction with an area of $1\,\mu m^2$ each, and also the studied signal transfer line matched with the antenna for input and SIS junctions for output. The twin SIS junctions instead of single SIS junctions are used to enlarge the width of receiving bandwidth due to mutual tuning out of the junctions capacity by means of inductance of the line which connects them. The detectors are included in sections of the microstrip line $\lambda/4$ and $3\lambda/4$, where λ — is the wavelength of received emission (further — short and long sections, respectively). The difference between the power received by the detector in long and short sections allow further assessment of losses in the microstrip line and defining the parameters of thin films. The integrated circuit is placed in focus of the semi-elliptic silicon lens which forms a quasi-optical antenna-to-lens receiving path.

Results of detected power calculations P_a in the short and long sections are given in Figure 2. The computational modeling method for these structures is described in details in [12], all calculations were performed in Ansys HFSS program. Frequency of the most efficient detection practically coincides for the two sections with an accuracy of 10 GHz and makes about 0.93 THz. At the same time the detected power in the long section near 1.1 THz frequency is practically by an order (8 dB) lower than in the short section which is illustrated by dotted line.

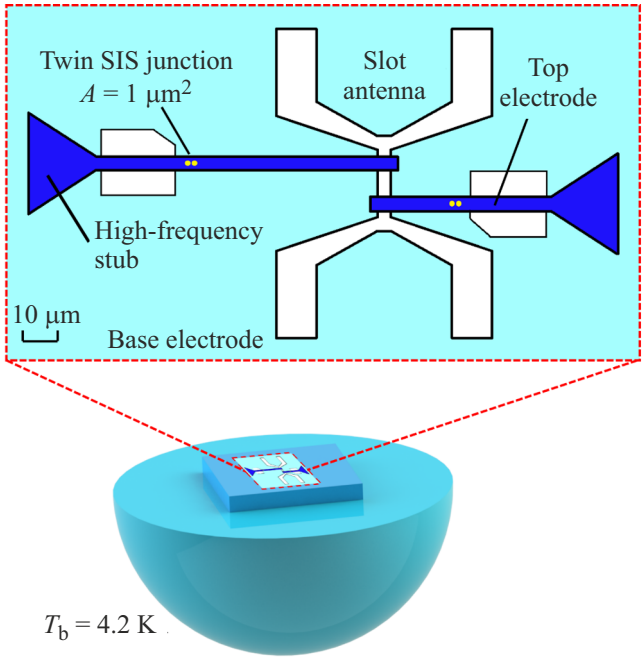

Figure 1. Topology of a superconductor integrated circuit for the study of absorption in NbTiN/Al (upper picture) signal transfer lines and layout of the chip placement on a lens to form a receiving path (lower picture).

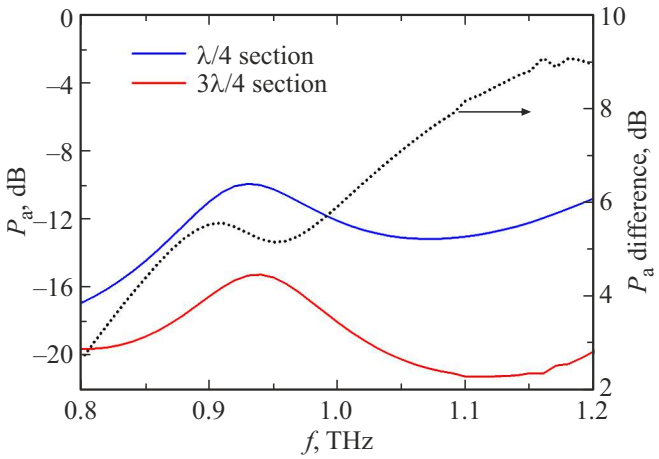

Figure 2. Results of detected power calculations in long and short sections and difference between them.

The prototypes of integrated circuits with a topology described above are made by methods of magnetron sputtering and optical UF-lithography, the photo templates with a submicron accuracy were manufactured using the e-beam lithography. All structures were manufactured using a high-resistance substrate ($> 5\,k\Omega \cdot cm$) of polished silicon. The manufacturing technology for Nb/AlN/Nb, Nb/AlN/NbN tunnel junctions using conventional Nb/Nb signal transfer lines is described in details in [13], whereas the tunnel junctions built in NbTiN/Al signal transfer lines were discussed in [14]. The micro-photos of the manufactured structures can be found in recent papers [8,12]. Normal resistance of junctions in short and long sections was equal 14.1 and 14.8 Ω respectively, which is less than a 5% difference and indicates a pretty high process accuracy in manufacture of structures with sizes of $1\,\mu m$.

3. Experiment of recording of THz-signal

The layout of the experimental device is shown in Figure 3. A cryogenic module with an integrated structure was placed in vacuum filled cryostat with an operating temperature of 4.2 K. A powerful BWT-based source with an operating frequency bandwidth of 0.9–1.1 THz was used as an outer generator to pump the SIS detectors with THz signal and study the properties of the signal transfer lines. BWT has an output frequency of 1.056 THz with a decelerating voltage on the cathode of 5 kV and frequency tuning ratio about 79GHz/kV, with generation occurring in 4–6 kV range. The action of THz signal of BWT on detector was recorded by measuring the current-

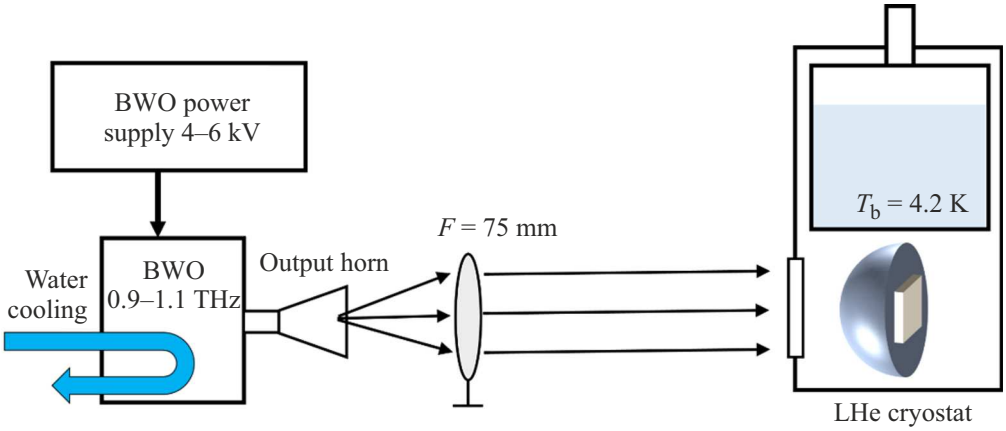

Figure 3. Layout of an experimental device for studying the pumping of SIS detectors with BWT signal at frequencies of up to 1.1 THz.

voltage curves (CVC) of the SIS junction. The characteristic currents through the junction were up to 1000 μA. To compensate for divergence of the source outgoing beam a collecting lens with a focal distance of 75 mm was placed; the lens is made of Teflon which is transparent in THz band.

Families of measured current-voltage curves of the SIS junctions for specific set of BWT operating parameters are given in Figure 4. The current-voltage curves in Figure 4, *a, b*, obtained with the specified number of BWT operating point, were measured simultaneously and independently on different detectors, at that, such a set of curves was selected for convenience as to demonstrate the possibility of SIS detectors pumping in a wide power range: from the pumping current of 0.1–0.2 of the „slot“ spike to the pumping saturation values). Various level of pumping power at one frequency of 1.130 THz (for operating points ## 1, 5, 7) was obtained by additional installation of one and two absorber layers. The insert windows in Figure 4, *a, b* illustrate the superconducting slot of the SIS junction to large scale, where it is seen that the slot value is greatly reduced with the pumping power growth; these results will be used to analyze the thermal effect in section 4.

If a SIS detector was exposed to outer emission without suppression of the critical current this will result in two series of tunnel current stages: Shapiro stage [15] and quasi-particle current stages [4]. For all curves of detectors exposed to emission in Figure 4, *a, b* a clear first Shapiro stage is observed for voltages in the range of 2–2.25 mV, and also a slight second stage on the normal section of the current-voltage curve under voltages of 4–4.5 mV. Position of stages exactly matches the source frequency 0.998–1.13 THz when Josephson constant is recalculated $2e/h \approx 483.6$ GHz/mV, where e — electron charge, h — Planck's constant.

Thus, a powerful pumping of detectors in both sections was obtained in BWT generation band 990 GHz to 1.13 THz, which demonstrates the applicability of the manufactured signal transfer lines for the detection purposes at these frequencies. In terms of quality the experimental

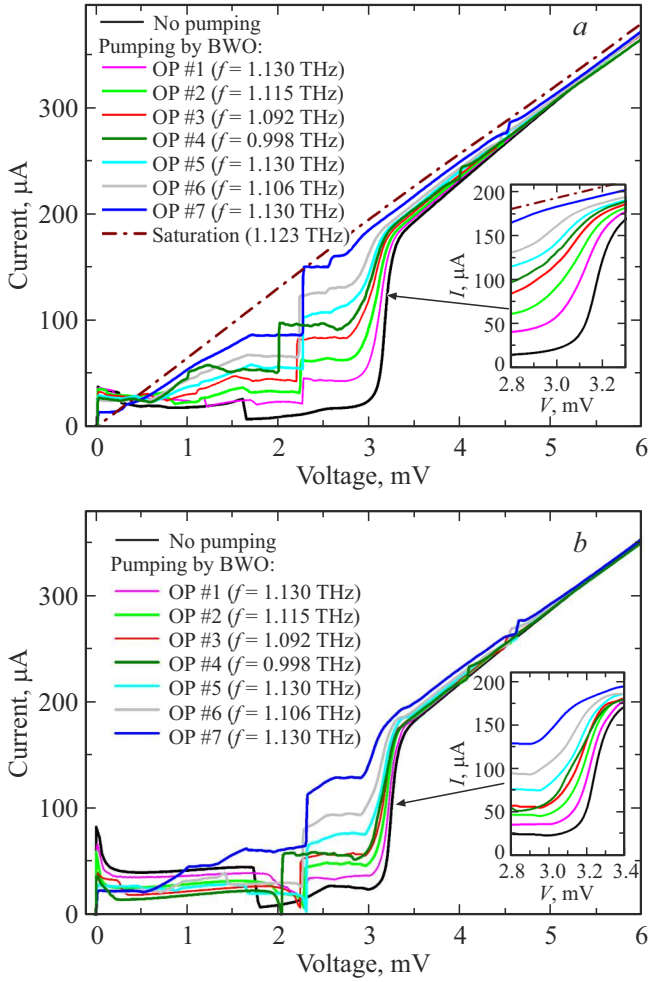

Figure 4. Series of current-voltage curves of SIS detectors in short (*a*) and long (*b*) sections without exposure and with exposure to the outer source signal of various power and frequencies. BWT parameters in operating points (OP) designated by the same number ## 1–7 are identical for (*a*) and (*b*).

data correspond to the quantitative data where pumping in the long section turned to be less efficient than in the shorter one. The VHF power absorbed by a SIS detector is commonly estimated by a computational modeling of a current-voltage curve under the action of emission (of certain power and frequency) and its comparison with experimentally measured current-voltage curve [4,9,10]. In its turn, to calculate the current-voltage curve under the action of emission it is required to know exact junction parameters independently (w/o exposure), including: normal transition resistance, gap voltage V_g and a „sub-slot“ current (leak current) I_{leak} at certain bias voltage. From insert windows in Figure 4, *a, b* it is seen that V_g is decreasing with the growth of pumping power which is first of all explained by thermal heating of the junction to some efficient temperature T_{eff} [9], while it is impossible to determine exact value V_g for the current-voltage curve shape under emission, since the CVC shape and slope in the „slot“ area is unknown because of extremely high quasi-particle stage. Moreover, experimental value of quasi-particle pumping current I_p for correct comparison with the numerical value is also unknown: first of all, Shapiro stages make a significant contribution to the characteristic shape (superposition of current stages of two independent effects), second, the leak current I_{leak} also depends on the junction temperature and is unknown under current junction temperature T_{eff}. In case of fully depressed critical current the pumping current is defined as an actual bias current through the junction I_{bias} and leak current $I_p = I_{\text{bias}} - I_{\text{leak}}$, however, in the applied measurement system there's no possibility to suppress critical current. Thus, a whole number of unknown parameters doesn't allow making a computational modeling with a verified result. To define V_g and I_{leak} for the quantitative assessment of power an additional research was carried out described in section 4.

4. Analysis of SIS detector pumping thermal effect

To determine the superconducting slot V_g and leak current I_{leak} of SIS detectors exposed to emission the independent measurements of current-voltage curves were carried out for a wide temperature range. This method was suggested and described in [9]. For this purpose, close to the integrated circuit a heating resistor component was placed with resistance of about 1 kΩ. Figure 5 illustrates a series of SIS junction current-voltage curves in the short section at various heating level: voltage fed to the heater element V_h was 8 V, with further increase of heating the shape of current-voltage curve becomes practically linear which indicates a temperature close to the critical temperature transition to normal state. A series of current-voltage curve looks practically identical to the junction in the long section since the junctions temperature is absolutely equal in both sections and is equal to the microcircuit temperature.

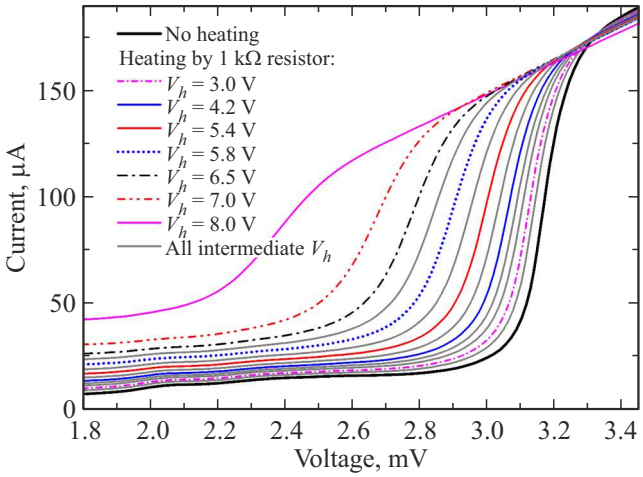

Figure 5. Series of SIS junction current-voltage curve in the short section under various temperatures which depend on voltage supplied to the heated component. For convenience the heater voltage is designated only for some curves with a spacing of about 1 V.

After that the current-voltage curve without exposure to outer signal corresponding to the same T_{eff} resulted from the heating from signal exposure is determined by comparing the curves. Thus, for detectors in the long section as seen from Figure 6, *b* it is established that for pumping with BWT signal in the operating point OP 1 the $V_g = 3.21$ mV, OP #2 — $V_g = 3.17$ mV, OP #3 — $V_g = 3.15$ mV, OP #5 — $V_g = 3.11$ mV, OP #6 — $V_g = 3.04$ mV, is best suited, at that V_g in the independent mode is 3.24 mV. Similarly, V_g were defined for various CVC curves with BWT signal pumping for a detector in the short section. Summary data of the gap voltage ΔV_g variation due to the detectors pumping for a set of studied points (source parameters) are given in Table.

The results given in the Table fully comply with visual comparison of the pumping power in the short and long sections (in terms of pumping stage height): with the given source parameters variation of the gap voltage ΔV_g of the SIS detector in the short section is higher than in the long section. It should be noted that this method for determination of V_g is applicable for pumping the SIS junction away from the saturation mode, when I_p makes no more than $\sim 0.7-0.8$ of the full current slot step. The near margin zone of the method applicability can be demonstrated, for instance, in Figure 6, *a* by the pumping curve for OP 5 and by appropriate curve at $V_h = 5.8$ mV, while in Figure 6, *b* it is demonstrated by the pumping curve for OP 6 and its appropriate curve $V_h = 5.2$ mV. For both cases, the current-voltage curve under the action of heating is not imposed directly on the pumping current-voltage curve, but rather it represent its visual extension with the same slope of the superconducting slot. For pumping close to saturation, e. g., as seen in Figure 6, *a* for the source operating points OP 6 and OP 7 it is practically impossible

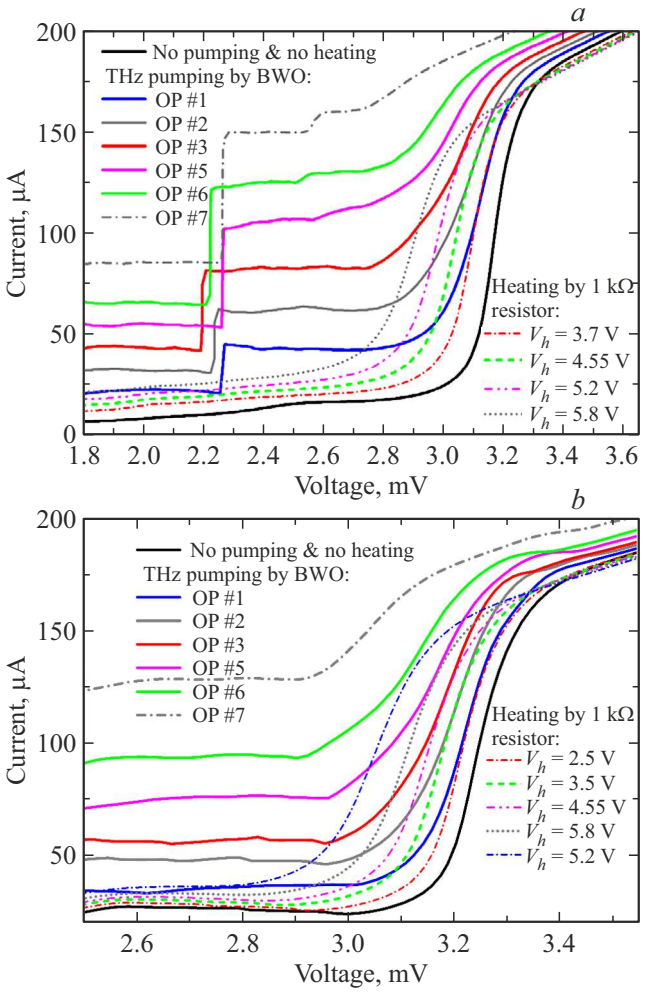

Figure 6. Results of comparing the current-voltage curve for SIS detector exposed to outer signal with the current-voltage curve with heating and without exposure to outer signal (a) for a SIS detector in short section, (b) — in long section.

Variation of detectors gap voltage versus pumping parameters

Operating point source	Frequency pumping, THz	ΔV_g of SIS detector, mV	
		in short section	in long section
OP #1	1.13	0.07	0.03
OP #2	1.115	0.13	0.07
OP #3	1.092	0.19	0.09
OP #5	1.13	0.25	0.13
OP #6	1.106	–	0.2

to determine V_g in this way. Therefore there's a blank space in the appropriate cell in the Table.

This method also allows to determine the leak current I_{leak} that can be seen directly from the experimental curve exposed to heating in the voltage range below the „slot“ (see Figure 5). It is interesting to note that it is not required to determine absolute value T_{eff} in this method, it is enough to achieve the appropriate heating of the SIS junction in the experiment. Determination of exact temperature is an separate numerical task to find $V_g(T) = \Delta_1(T) + \Delta_2(T)$ (a sum of superconducting gaps of SIS junction electrodes) with boundary conditions. This task within this research. Power produced by resistor within the context of this research is also of no importance, since there's no need to solve the three-dimensional problem of heat conductance in the detector heating system.

5. Conclusion

The superconducting integrated structures based on SIS detectors are the highly sensitive receiving systems both, in sub-THz range, and at frequencies above 1 THz, however, the design of signal transfer lines and their improvement for specific tasks is quite a complex technological and computational issue. This paper outlines the process of development, numerical simulation, manufacture and experimental testing of an integrated structure based on receiving antenna and SIS detectors Nb/AlN/NbN integrated with NbTiN/Al signal transfer line with operating frequency band of 0.9−1.1 THz. As an outer THz-emission source the backward-wave oscillator was used with quasi-optical antenna-lens path as a feeder. Thus, a powerful pumping of SIS detectors in 0.998−1.13 THz band was obtained, which demonstrates successful functioning of the designed SIS junctions and signal transfer lines for operation at target frequency of above 1 THz. A method was tested for determination of gap voltage and leak current for a SIS detector exposed to powerful outer emission, for which an additional experiment with the junction heating was used. The applied method for determination of electrophysical parameters of detector, as well as suppression of critical current allows further calculating the detectors pumping power in absolute units, at that, the difference of this power in short and long sections will enable us to define the damping parameter in the NbTiN/Al microstrip signal transfer line.

Acknowledgments

All samples were made using a unique scientific plant „Criointegral“ (UNU No. 352529) of the Radio-engineering and Kotelnikov Institute of Radioengineering and Electronics (IRE) of Russian Academy of Science.

Funding

The study was carried out with the financial support of the Ministry of Science and Higher Education of Russia (agreement No. 075-15-2024-538).

Conflict of interest

The authors declare that they have no conflict of interest.

References

[1] S.L. Dexheimer. Terahertz Spectroscopy: Principles and Applications. CRC Press, N.Y. (2008). 360 p.
[2] D.F. Plusquellic, K. Siegrist, E.J. Heilweil, O. Esenturk. Chem. Phys. Chem. **8**, *17*, 2412. (2007).
[3] A.G. Davies, A.D. Burnett, W. Fan, E.H. Linfield, J.E. Cunningham. Mater. Today **11**, *3*, 18 (2008).
[4] J.R. Tucker, M.J. Feldman. Rev. Mod. Phys. **57**, *4*, 1055 (1985).
[5] D.C. Mattis, J. Bardeen. Phys. Rev. **111**, *2*, 412 (1958).
[6] J.W. Kooi, J.A. Stern, G. Chattopadhyay, H.G. LeDuc, B. Bumble, J. Zmuidzinas. Int. J. Infrared Millimeter Waves **19**, *3*, 373 (1998).
[7] B.D. Jackson, N.N. Iosad, G. Lange, A.M. Baryshev, W M. Laauwen, J.R. Gao, T.M. Klapwijk. IEEE Trans. Appl. Supercond. **11**, *1*, 653 (2001).
[8] N.V. Kinev, A.M. Chekushkin, F.V. Khan, K.I. Rudakov. Radiotekhnika i elektronika, **68**, *9*, 858 (2023). (in Russian).
[9] A. Traini, B.K. Tan, J.D. Garrett, A. Khudchenko, R. Hesper, A.M. Baryshev, P.N. Dmitriev, V.P. Koshelets, G. Yassin. IEEE Trans. THz Sci. Technol. **10**, *6*, 721 (2020).
[10] N.V. Kinev, K.I. Rudakov, L.V. Filippenko, A.M. Baryshev, V.P. Koshelets. Sensors **20**, *24*, 7276 (2020).
[11] A. Khudchenko, A.M. Baryshev, K. Rudakov, V. Koshelets, P. Dmitriev, R. Hesper, L. Jong. IEEE Trans. THz Sci. Technol. **6**, *1*, 127 (2016).
[12] N.V. Kinev, A.M. Chekushkin, F.V. Khan, V.P. Koshelets. In Proc.: 2023 Radiation and Scattering of Electromagnetic Waves (2023). P. 128.
[13] P.N. Dmitriev, I.L. Lapitskaya, L.V. Filippenko, A.B. Ermakov, S.V. Shitov, G.V. Prokopenko, S.A. Kovtonyuk, V.P. Koshelets. IEEE Trans. Appl. Supercond. **13**, *2*, 107 (2003).
[14] A.M. Chekushkin, L.V. Filippenko, M.Yu. Fominsky, V.P. Koshelets. FTT **64**, *10*, 1399 (2022). (in Russian).
[15] C.C. Grimes, S. Shapiro. Phys. Rev. J. Archive **169**, *2*, 397 (1968).

Translated by T.Zorina